

# Diffusion-Limited Chemical Reactions in a Turbulent Shear Layer

Irwin E. Alber\* and Richard G. Batt†  
TRW Systems Group, Redondo Beach, Calif.

A probability density function (pdf) model is developed to analyze the effects of turbulent mixing on two diffusion-limited chemically reacting shear flow problems: 1) the dissociation of cold dilute  $N_2O_4$  within a shear layer mixing with warm room air,  $N_2O_4 + N_2 \rightleftharpoons 2NO_2 + N_2$ ; and 2) the isothermal turbulent diffusion flame formed by the reaction  $A + B \rightarrow C$  of initially unmixed reactants  $A$  and  $B$  brought together in a turbulent shear layer. Measured temperature probability density functions across the free mixing layer indicate that approximately the mid-50% of the shear layer is fully turbulent and nearly Gaussian in its statistics. By assuming such a single variate normal pdf for the equivalent inert species mixing field, the ensemble average and rms fluctuation levels of the products of the chemical reactions are calculated readily by a simple quadrature. The mean and variance of the pdf are calculated from shear layer similarity solutions for mean temperature  $\bar{T}$  and mean square temperature  $\bar{T'^2}$ . Comparisons of the theory are made with the  $NO_2$  data for the first-order dissociation problem.

## Nomenclature

$A, B$	= molar concentration of reactants on either side of shear layer
$C$	= molar concentration of product in reaction $A + B \rightarrow C$ , also denoted by $[C]$
$e$	= turbulent kinetic energy = $\frac{1}{2}(u'^2 + v'^2 + w'^2)$
$f(T)$	= probability density function for temperature
$k_D, k_R$	= dissociation and recombination constants
$K_p$	= equilibrium constant = $(1/RT)k_D/k_R$
$[NO_2], [N_2O_4]$	= molar concentration of $NO_2, N_2O_4$
$[N_2O_4]_a$	= $N_2O_4$ available for reaction = $[N_2O_4] + \frac{1}{2}[NO_2]$
$P$	= static pressure
pdf	= probability density function
$\frac{T}{\bar{T}^2}$	= temperature
$\bar{T'^2}$	= mean square temperature fluctuation
$\bar{u}, \bar{v}$	= mean velocity components in $x, y$ directions
$x, y$	= axial and transverse coordinates
$X_a$	= mole fraction available = $[N_2O_4]_a / [N_2]_1$
$\alpha$	= degree of dissociation = $1 - [N_2O_4] / [N_2O_4]_a$
$\Lambda$	= integral scale of turbulence
$\eta$	= shear layer similarity variable = $\sigma_u y / x$
$\rho$	= density
$\sigma_u$	= shear layer spreading parameter
$\tau_c, \tau_D$	= chemical and turbulent diffusion times

## Subscripts

$1, 2$	= denotes high- and low-speed edges of shear layer, respectively
$\infty$	= freestream conditions $A_\infty = A_1, B_\infty = B_2$

## I. Introduction

A WIDE variety of chemically reacting flow problems, currently under study by engineers, require the prediction of the mean and fluctuating species concentrations that result from chemical reactions taking place in turbulent shear layers. It can be shown that applying theories for first- and second-order chemical reactions, which have been developed for steady laminar flow problems, can lead to an overestimate of the amount of the reaction product flux for the turbulent case of initially unmixed reactants. The physical reason lies with the continuous random movement of the reaction zones in turbulent flow, as opposed to their stationary behavior in laminar flows.

This paper seeks to develop a simplified statistical model for the effects of inhomogeneous turbulent mixing on a chemically reacting flow by examining two prototype problems: 1) first-order reaction: the dissociation of highly diluted cold nitrogen tetroxide ( $N_2O_4$ ) within a turbulent free shear layer mixing with quiescent room temperature ambient air (Fig. 1a),  $N_2O_4 + N_2 \rightleftharpoons 2NO_2 + N_2$ ; and 2) second-order reaction: the turbulent diffusion flame formed by the reaction of initially highly diluted unmixed reactants  $A$  and  $B$ , which are brought together in a turbulent shear layer to form the product  $C$  by the one-step reaction (Fig. 1b),  $A + B \rightarrow C$ .

For all of the problems under study, the reactions are assumed diffusion-limited, i.e., the reaction time is much less than the turbulent diffusion time  $\tau_D$  ( $\tau_c \ll \tau_D$ ). For many reactions and flow conditions of interest, this assumption is quite valid. For example, this was the case in the  $N_2O_4$  dissociation mixing layer experiments of Batt,<sup>1</sup> where, as will be shown,  $\tau_c/\tau_D < 0.01$ . Hofland and Mirels<sup>2</sup> also have shown that the diffusion-limited assumption can be applied to the analysis of HF chemical lasers with dilute oxidizer flows.

The general method of solution adopted in this study for such diffusion-limited reactions can be termed to be a form of the turbulent ensemble or probability density approach. The present paper (edited from Ref. 3) is unique in that the ensemble analysis for the first time has been used to study a particular turbulent reaction flow (problem 1) for which complete detailed measurements of the fluctuating chemical

Presented as Paper 74-593 at the AIAA 7th Fluid and Plasma Dynamics Conference, Palo Alto, Calif., June 17-19, 1974; submitted July 17, 1974; revision received August 1, 1975. This work was sponsored by ARPA under Contract No. F0401-71-0040. The authors wish to acknowledge the fine numerical analysis and programming support of Elza Kampe.

Index categories: Jets, Wakes, and Viscid-Inviscid Flow Interactions; Reactive Flows; Combustion in Gases.

\*Principal Staff Engineer, Fluid Mechanics Department, Member AIAA.

†Staff Engineer, Engineering Sciences Laboratory, Member AIAA.

system are available. In addition to the present analysis, several similar statistical models have been developed by other researchers and applied to various types of reactive turbulence problems.<sup>4-7</sup>

All of these statistical theories either utilize a model equation for the local probability density function (pdf) or generate one from a local Gaussian hypothesis. The pdf form used in this study for the shear layer problem is discussed in Sec. II. The first-order  $N_2O_4$  dissociation problem then is analyzed, using the pdf model, in Sec. III. For this first-order problem, it is assumed that the reactions are very fast (diffusion-limited) and hence that an ensemble of temperature- $N_2O_4$  eddies still exists with a local equilibrium composition. The same basic analysis then is applied to the isothermal second-order chemical shear layer problem in Sec. IV. (see Fig. 1b), but the temperature probability distribution function is replaced with one for the equivalent inert species  $X \equiv A - B$ .

## II. Scalar Statistical Properties of Unreacting Shear Layers

Recently, Libby<sup>7</sup> used the probability density function (pdf) approach to study the two-dimensional mixing of two streams, each with one reactant present. He stressed the importance of turbulent intermittency  $\Omega$  in determining the shape of the pdf profile at different locations within the shear flow. By examining pdf data taken from measurements of the temperature within the wake of a heated cylinder, Libby has shown that, although the pdf is Gaussian on the wake centerline, highly skewed pdf are more typical off centerline in regions where  $\Omega < 1$ , i.e., where the interface structure contributes significantly to the scalar statistics. He used this wake pdf as a qualitative guide in developing several models for the pdf profiles for the reacting shear layer problem.

In Batt's shear layer studies,<sup>1</sup> he performed a series of hot-wire measurements of the scalar temperature field at different locations across the shear layer. His data on temperature pdf's across the shear layer (Fig. 2) indicate that a broad domain (approximately the mid-50% of the shear layer) is fully turbulent ( $\Omega \approx 1.0$  within a measurement uncertainty of 0.05) and nearly Gaussian in its statistics. The data do reveal a more one-sided pdf near the intermittent jet boundaries. These shear layer results contrast markedly with the relatively small fully turbulent domain ( $\Omega = 1$ ) in the wake of a cylinder. In addition, Batt's data show a significant difference between the statistical averages for the temperature and velocity fields. These quantities must be known accurately, particularly for the scalar field, in order to describe the scalar pdf in the fully turbulent zone. In regions where  $\Omega_T = 0(1)$ ,<sup>†</sup> it will henceforth

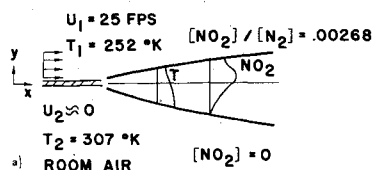


Fig. 1a First-order reaction turbulent mixing problem, dissociation  $N_2O_4 = 2NO_2$ .

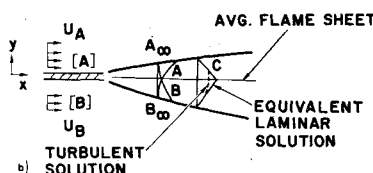


Fig. 1b Second-order reaction turbulent mixing problem,  $A + B = C$ .

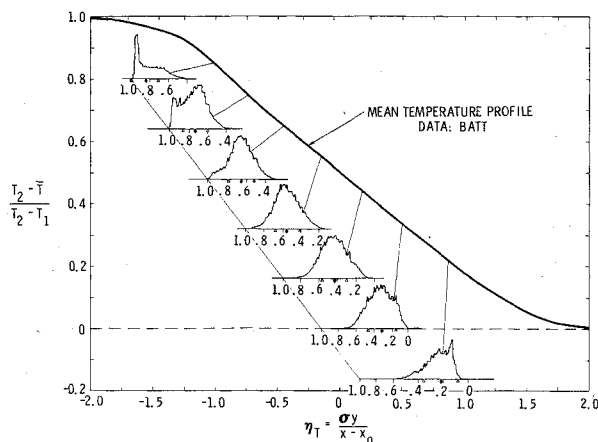


Fig. 2 Measured temperature probability density profiles at different locations across the shear layer. ( $\diamond$  = mean temperature,  $\Delta$  = standard deviation).<sup>1</sup>

be assumed that the pdf can be written simply in terms of its local mean and variance using the Gaussian formula

$$f(T) = [1/(2\pi\sigma_T^2)]^{1/2} \exp[-(T - \bar{T})^2 / 2\sigma_T^2] \quad (1)$$

where

$$\sigma_T = \overline{T'^2}$$

An earlier version of this paper<sup>3</sup> included an analysis of the mean and fluctuating properties of unreacting turbulent shear layers. Model equations developed for the turbulent kinetic energy and mean square fluctuating temperature  $\overline{T'^2}$ , when solved in conjunction with the mean energy equation for  $\bar{T}$ , provided the parameters needed in the Gaussian formula, Eq. (1). Direct comparisons with the temperature data verified the adequacy of the scalar model. The principal conclusions to be drawn from these scalar calculations are the following: 1) The mean temperature profile is nearly linear across the jet (see Fig. 2). 2) The rms temperature profile shows a plateau level of approximately 14 to 15% in the mid-3/4 of the shear layer, dropping off fairly rapidly to zero at the edges.<sup>§</sup>

This passive scalar information now can be used as input data for the Gaussian probability formula, Eq. (1), which will be employed in the calculations of the diffusion-limited reacting flow systems presented in Sec. III. and IV.

## III. First-Order Dissociation Reaction

The model diffusion-limited reactive flow problem (Fig. 1a), to be solved in this section by the pdf analysis, is the dissociation and recombination within a turbulent shear layer of highly diluted nitrogen tetroxide, which follows the chemical reaction



The  $[N_2O_4]$  is injected in small concentrations into a high-speed stream of cooled air at temperature  $T_1$  ( $\sim 252K$ ) before entering the mixing layer. In the cool freestream, the  $[N_2O_4]$  dissociates a small amount, forming an ambient level of  $[NO_2]$  in the air carrier gas, the degree of dissociation  $\alpha_1$  being on the order of 37% for  $T_1 = 252K$ . The degree of dissociation is defined as

$$\alpha = 1 - \frac{[N_2O_4]}{[N_2O_4]_a} = \frac{1}{2} \frac{[NO_2]}{[N_2O_4]_a} \quad (3)$$

<sup>†</sup> When it is stated that  $\Omega = 0(1)$ , we refer to an intermittency based only on the measured temperature signal.

<sup>§</sup> The experimental data of Batt<sup>1</sup> indicates a slight double peak in  $\overline{T'^2}$  (c.f. Fig. 6) not predicted in the calculations of Ref. 3.

In Eq. (3),  $[N_2O_4]_a$  is the total amount of  $[N_2O_4]$  available for reaction and is defined by the relation

$$[N_2O_4]_a \equiv [N_2O_4] + \frac{1}{2}[NO_2] \quad (4)$$

As will be shown,  $[N_2O_4]_a$  is a reaction invariant and depends only on the turbulent transport properties.

#### A. Species Conservation Equation

The governing conservation equations for the molar concentrations  $[N_2O_4]$  and  $[NO_2]$  for the mixing layer with dissociation-recombination reactions are

$$\begin{aligned} \frac{\partial [N_2O_4]}{\partial t} + \frac{\partial}{\partial x} (\bar{u}[N_2O_4]) + \frac{\partial}{\partial y} (\bar{v}[N_2O_4]) \\ = -\dot{\omega} + \frac{\partial}{\partial y} \left[ D \frac{\partial [N_2O_4]}{\partial y} \right] \end{aligned} \quad (5)$$

$$\begin{aligned} \frac{\partial [NO_2]}{\partial t} + \frac{\partial}{\partial x} (\bar{u}[NO_2]) + \frac{\partial}{\partial y} (\bar{v}[NO_2]) \\ = 2\dot{\omega} + \frac{\partial}{\partial y} \left[ D \frac{\partial [NO_2]}{\partial y} \right] \end{aligned} \quad (6)$$

where  $\dot{\omega}$  = rate of dissociation minus the rate of recombination, units of moles per square centimeter-second:

$$\dot{\omega} = k_D [N_2O_4] [N_2] - k_R [NO_2]^2 [N_2] \quad (7)$$

where

$$k_D = \text{rate constant for dissociation} = 2 \times 10^7 \exp(-5550/T) \text{ cm}^3/(\text{mole} \cdot \text{sec})^8$$

$$k_R = \text{recombination rate constant} = 1.64 \times 10^{10} T \exp(1200/T) \text{ cm}^6/(\text{mole}^2/\text{sec})$$

By adding one-half of Eq. (5) to Eq. (6), one obtains the governing equation for the reaction invariant  $[N_2O_4]_a$ , defined by Eq. (4)

$$\begin{aligned} \frac{\partial}{\partial t} [N_2O_4]_a + \frac{\partial}{\partial x} (\bar{u}[N_2O_4]_a) + \frac{\partial}{\partial y} (\bar{v}[N_2O_4]_a) \\ = \frac{\partial}{\partial y} \left[ \hat{D} \frac{\partial [N_2O_4]_a}{\partial y} \right] \end{aligned} \quad (8)$$

Note that Eq. (8) does not contain the production term  $\dot{\omega}$ .

Rewriting Eq. (8) in terms of the mole fraction  $X_a \equiv [N_2O_4]_a/[N_2]$ , and then performing the usual turbulent time averages, one finds the following diffusion equation for the mean mole fraction  $\bar{X}_a$

$$\bar{u} \frac{\partial \bar{X}_a}{\partial x} + \bar{v} \frac{\partial \bar{X}_a}{\partial y} = \frac{1}{\bar{\rho}} \left[ \bar{D} \frac{\partial \bar{X}_a}{\partial y} - \overline{\bar{\rho}(v'X'_a)} \right] \quad (9)$$

The density fluctuation terms  $\overline{v'\rho'}$ ,  $\overline{X'\rho'}$  have been neglected in Eq. (9) (for low-speed flows) compared to the turbulent diffusion flux term  $\bar{\rho}(v'X'_a)$ . Equation (9) is identical to the mean energy equation for mean temperature  $\bar{T}$  if one makes the following assumptions: 1)  $\partial \bar{\rho}/\partial y$  terms are small compared to  $\partial/\partial y (\bar{\rho}X'_a)$  across the shear layer, 2) molecular diffusions are small compared to those for turbulent diffusion, and 3) the turbulent Schmidt and Prandtl numbers are the same (unity turbulent Lewis number). Equation (8) is, in fact, identical to the instantaneous thermal transport equation un-

der assumptions 1 and 2. Hence, the shear layer normalized solutions for temperature and mole fraction can be equated

$$X_a/X_{a1} = (T_2 - T)/(T_2 - T_1) \quad (10)$$

#### B. Time Scales for Species Chances

Chemical nonequilibrium effects will be important in the solution of Eqs. (5) and (6), provided that the characteristic time scale  $\tau_c$  for concentration changes due to chemical reactions is of the order of the time scale  $\tau_D$  for turbulent diffusion of the dominant eddies. Characteristic time scales for chemical dissociation and recombination, based on an average temperature of 265K, are quite small, of the order of  $10^{-4}$  sec. The time scale associated with turbulent diffusion based on integral scale size eddies,  $\tau_D = \Lambda/u'$ ,  $\approx 0.05$  sec ( $\Lambda$  = integral scale of turbulence), is more than two orders of magnitude larger than the characteristic time for dissociation or recombination,  $\tau_c$ . It is only when one examines the time scales associated with the smallest scale eddies, those characteristic of turbulent dissipation, that there appears any possibility for nonequilibrium effects under conditions corresponding to Batt's experiments.<sup>†</sup>

#### C. Quasi-equilibrium Results

Since  $\tau_c \ll \tau_D$ , one can assume that the eddy constituents undergo forward and backward reactions so rapidly that they are in a state of local equilibrium; the local equilibrium  $NO_2$  mole fraction is given by

$$[NO_2]/[N_2] = (Kp/4P) \{ [1 + (16PX_a/K_p)] \}^{1/2} - 1 \quad (11)$$

where

$$X_a/X_{a1} = (T_2 - T)/(T_2 - T_1)$$

The measured equilibrium constant for  $N_2O_4 \rightleftharpoons 2NO_2$  is, from Bodenstein and Boes,<sup>9</sup>

$$K_p = RT(k_D/k_R) = \exp[20.72 - (6747/T)] \text{ atm.}$$

$NO_2$  mole fraction, plotted as a function of temperature, is presented in Fig. 3 for the  $T_1 = 252K$  case and for a range of lower freestream temperatures. In Fig. 3, the solid lines denote shear layer profiles of the mean  $NO_2$  mole fraction, calculated from Eq. (11), using the local mean temperature  $\bar{T}$ . One notes that the magnitude of the peak in the local  $[NO_2]$  concentration increases (relative to its freestream value) as the freestream temperature  $T_1$  decreases. The calculation for the case  $T_1 = 220K^{**}$  shows a peak in  $[NO_2]$  mole fraction more than five times its freestream value. As noted previously, the  $NO_2$  concentration falls rapidly from this peak as  $(\bar{T} - T_1)/(T_2 - T_1) \rightarrow 1$ , because of the continual decrease in the available  $N_2O_4$  in regions where the degree of dissociation  $\alpha$  is near unity (i.e., on the high-temperature side of the jet). For the case  $T_1 = 252K$ , where Batt made his  $[NO_2]$  measurements, the peak  $[NO_2]$  ratio, based on the local mean temperature, is approximately 1.3 times the freestream value,  $\{[NO_2]/[N_2]\}_1$ .

The local ensemble, or time-averaged concentration of  $NO_2$ , defined as  $\langle NO_2 \rangle$ , will not have as large a peak as one would calculate based on shear layer mean temperature properties. This reduction in the peak can be explained by the following argument. Consider that one is viewing the chemical concentrations of the eddies passing a given point near the region where  $[NO_2](\bar{T})$  is a maximum. At this location, one will see eddies with temperatures near the mean,

<sup>†</sup>The midjet integral scale of the moving frame autocorrelation for temperature measured by Batt<sup>1</sup> is approximately 0.045 sec ( $u_1 = 23$  fps); for velocity it is 0.03 sec.

<sup>\*\*</sup>This case,  $T_1 = 220K$ , may not be physically realizable as condensation effects become important at these low temperatures.

colder than the mean, and warmer than the local mean. Those whose temperatures differ significantly from the mean will have  $\text{NO}_2$  concentrations below the peak value, whether they are hot or cold. Hence, when one forms averages based on all of the possible eddy temperature states passing a given point, the peak ensemble average will, of necessity, be decreased over what it would be based on the local mean temperature.

Such an ensemble mean,  $\langle [\text{NO}_2]/[\text{N}_2] \rangle$ , can be calculated readily from the following equation for the first concentration moment of the probability density function  $f(T)$

$$\left\langle \frac{[\text{NO}_2]}{[\text{N}_2]} \right\rangle = \int_{-\infty}^{\infty} \frac{[\text{NO}_2]}{[\text{N}_2]}(T) \cdot f(T) dT \quad (12)^{\dagger\dagger}$$

In the preceding integral,  $[\text{NO}_2]/[\text{N}_2]$  is given as a function of temperature by Eq. (11). As a first estimate for the form of the probability density function to be used in Eq. (12), it is assumed that  $f(T)$  is given by the Gaussian formula, Eq. (1). Numerical calculations of Eq. (12), using the calculated values of  $T'^2$  from Ref. 3, have been carried out for a range of freestream temperatures  $T_1$ . The resultant  $\text{NO}_2$  profiles are shown in Fig. 3 as the dashed lines. It is seen that the peak values of  $\text{NO}_2$  are reduced from the mean calculations by about 15% at the lower  $T_1$  conditions ( $T_1 = 220\text{K}$ ) but only about 5% at the  $T_1 = 252\text{K}$  experimental condition. The small reduction at the  $T_1 = 252\text{K}$  condition is due to the very flat profile for  $\text{NO}_2(T)$  near the high-speed side of the jet. Thus, for  $T_1 = 252\text{K}$ , most eddies, near the peak, have much the same concentration of  $[\text{NO}_2]$ , even though they have considerably different temperatures. The results are more evident in Fig. 4, where both the mean and ensemble analysis are shown in comparison with Batt's mean  $\text{NO}_2$  data. These  $\text{NO}_2$  data were obtained with the use of a small fiber optics probe positioned at different points in the flow. The uncertainty in the data is between 10 and 15%. The agreement between the ensemble average calculation and the data is fair, but the comparison is not conclusive as to the significance of the ensemble average procedure.

A much more definitive demonstration of the power and simplicity of the ensemble technique is the calculation of the rms concentration fluctuation,  $([\text{NO}_2]'^2)^{1/2}$ . This concentration intensity is calculated readily from the second moment of the concentration distribution.

The calculated profiles of rms concentration across the jet are shown in Fig. 5 for several values of the freestream temperature, and in Fig. 6 comparisons between the theoretical results and Batt's rms concentration data are displayed for the particular case  $T_1 = 252\text{K}$ . One can see immediately from Figs. 5 and 6 the very large concentration intensities that develop within the shear layer, values ranging from 30% to more than 100% of the freestream concentration. These rms concentration levels are considerably greater than the corresponding scalar intensities for temperature  $(T'^2)^{1/2} (\approx 15\%)$  and increase in magnitude with decreasing freestream temperature  $T_1$ . The agreement between theory and data as to the magnitude and form of the concentration intensity profiles (Fig. 6) is quite good over most of the jet, with some disagreement near the low-speed edge, where  $[\text{NO}_2]'$  peaks. The measured rms level at this point is about 40%, whereas the calculated value is approximately 30%.

#### IV. Second-Order Chemical Reactions

In this section, the model problem to be investigated with the ensemble average approach is the mixing and reaction of dilute reactants  $A$  and  $B$  to form the product  $C$  in an incompressible isothermal turbulent shear layer, as shown in Fig. 1b. The reaction between the two species again is assumed diffusion-limited, i.e.,  $\tau_c/\tau_D \ll 1$ , and follows the

<sup>††</sup> Bilger<sup>10</sup> has proposed a similar expression for equilibrium turbulent diffusion flames.

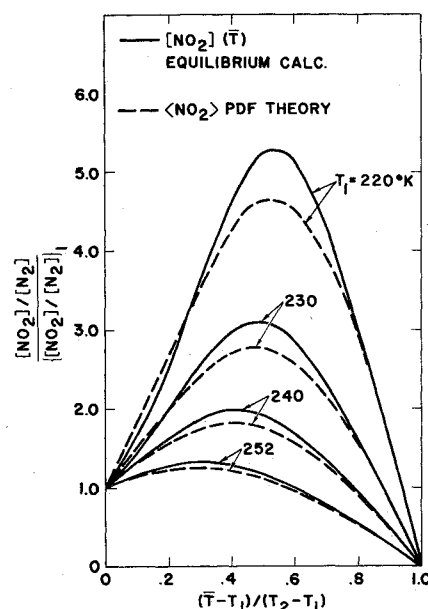


Fig. 3 Calculated mean mole fraction of  $\text{NO}_2$ .

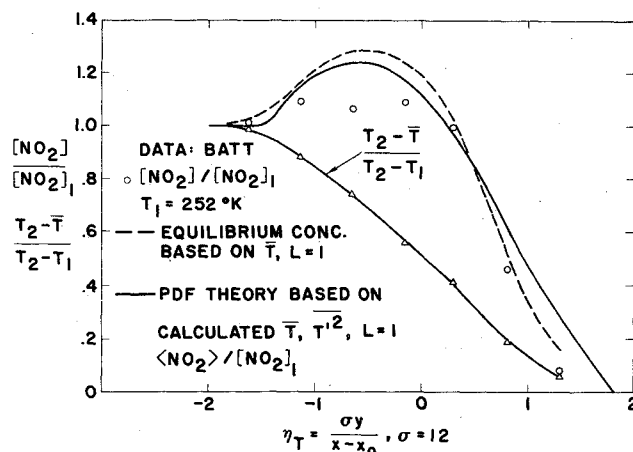


Fig. 4 Mean mole fraction profiles of  $\text{NO}_2$ . Comparison of mean equilibrium and ensemble average theory with Batt data ( $T_1 = 252\text{K}$ ).

one-step relation



##### A. Species Conservation Equations

The governing conservation equations for the molecular concentration  $A \equiv [A]$ ,  $B \equiv [B]$ , and  $C \equiv [C]$  for the incompressible layer are

$$(DA/Dt) - D_A \nabla^2 A = -\dot{\omega} \quad (14)$$

$$(DB/Dt) - D_B \nabla^2 B = -\dot{\omega} \quad (15)$$

$$(DC/Dt) - D_C \nabla^2 C = \dot{\omega} \quad (16)$$

where  $\dot{\omega}$  = chemical reaction rate  $= k(A \cdot B)$ ;  $k$  = reaction rate constant;  $D/Dt$  = substantive derivative  $= \partial/\partial t + \mathbf{u} \cdot \nabla$ ;  $D_A$ ,  $D_B$ ,  $D_C$  = molecular diffusivities of each constituent. It is shown readily for equal diffusivities (or when laminar effects are negligible) that one can obtain a reaction-invariant solution of Eqs. (14-16) for the variables

$$X = A - B \quad (17)$$

$$\psi = A + C \quad (18)$$

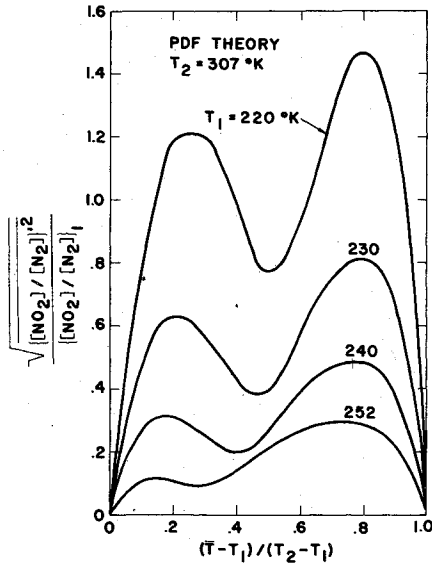


Fig. 5 Calculated  $\text{NO}_2$  mole fraction intensity profiles for various freestream temperatures  $T_1$ .

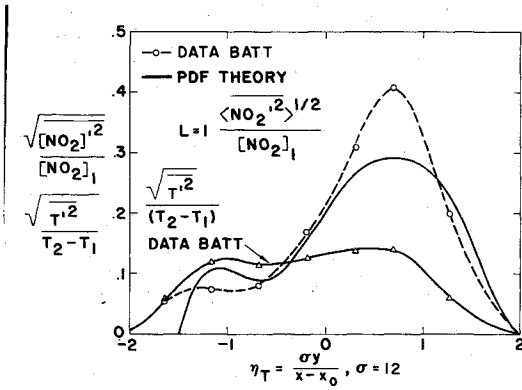


Fig. 6  $\text{NO}_2$  intensity profiles. Comparison of probability theory with data of Batt ( $T_1 = 252\text{K}$ ). Also includes measured temperature intensity profiles.

Each of the variables  $X$  and  $\psi$  thus satisfies a scalar diffusion equation of the form given by Eq. (8) for  $[\text{N}_2\text{O}_4]_a$ . Since the governing diffusion equations for  $X$  and  $\psi$  are independent of the reaction rate  $\omega$ , their solutions depend only on the statistics of the turbulent velocity field. Alternate measurements of the statistics of equivalent scalar quantities, such as temperature, also provide a representation of the solutions for  $X$  and  $\psi$ .

The time or ensemble-average solutions for  $X$  and  $\psi$  in a turbulent shear layer are represented analytically by

$$(\langle X \rangle + B_\infty) / (A_\infty + B_\infty) = \psi / A_\infty = \phi(\eta) \quad (19)$$

As noted in Sec. II.,  $\phi(\eta)$  is nearly linear across the shear layer and hence can be written in the following form:

$$\phi(\eta) = (\eta_2 - \eta) / (\eta_2 - \eta_1) \approx (1.6 - \eta) / 3.0 \quad (20)$$

## B. Diffusion-Limited Reaction

To determine the reactants  $A$  and  $B$  and the product  $C$  from the solutions for  $\psi$  and  $X$  requires either a solution of Eq. (14) or an assumption concerning the behavior of the individual constituents  $A$  and  $B$ . For the limiting case of an infinitely fast reaction, one can show that, at points in the flow where  $A$  exists,  $B=0$ , and where  $B$  exists  $A=0$ , so that no reactions occur except at the interfaces between  $A$  and  $B$ , i.e., in reaction zones with molecular dimensions.

Following O'Brien,<sup>4</sup> since  $A \geq B$ ,  $B \geq 0$ , and  $AB \rightarrow 0$  for very rapid reactions, the physical statement that if  $A > 0$ ,  $B=0$ , and if  $B > 0$ ,  $A=0$  leads to the following relations among  $A$ ,  $B$ , and  $X$ :

$$\text{if } X > 0, \quad A = X \quad B = 0 \quad (21)$$

$$\text{if } X < 0, \quad A = 0 \quad B = -X \quad (22)$$

In terms of  $\psi$ , since  $C = \psi - A$ , one finds that

$$\text{if } X > 0, \quad C = \psi - X$$

$$\text{if } X < 0, \quad C = \psi \quad (23)$$

Note that the ensemble average of the reaction product  $\langle C \rangle$  is determined directly from the solution for the ensemble average for the reactant  $A$  by

$$\langle C \rangle = \langle \psi \rangle - \langle A \rangle \quad (24)$$

Similarly, for the reactant  $B$ ,

$$\langle B \rangle = \langle A \rangle - \langle X \rangle \quad (25)$$

The ensemble average  $\langle A \rangle$  is determined readily from the integral expressing the conditional ( $X > 0$ ) expected value for  $X$ :

$$\langle A \rangle = \int_{-\infty}^{\infty} A(X) f(X) dX = \int_0^{\infty} X f(X) dX \quad (26)$$

In Eq. (26), use has been made of the diffusion-limited conditions given by Eqs. (21) and (22).

The pdf,  $f(X)$ , which adequately represents the passive scalar mixing process throughout the midportion of the free shear layer, again is assumed to be Gaussian, i.e.,

$$f(X) = [1 / (2\pi\sigma_X^2)]^{1/2} \exp[-(X - \bar{X})^2 / 2\sigma_X^2] \quad (27)$$

where  $\bar{X} = \langle X \rangle$  and  $\sigma_X^2 =$  variance of  $X \equiv \langle X'^2 \rangle$ . Note that Eq. (26) is valid for diffusion-limited flows regardless of the form chosen for the pdf. The rms intensity  $\sigma_X$  can be expressed in terms of a relative intensity based on the overall scalar potential ( $X_{\max} - X_{\min}$ ) by

$$\begin{aligned} \sigma_X &= [\langle X'^2 \rangle / (X_{\max} - X_{\min})] (X_{\max} - X_{\min}) \\ &\equiv \sigma_\psi (A_\infty + B_\infty) \end{aligned} \quad (28)$$

The relative intensity  $\sigma_\psi$  is equivalent to the nondimensional rms temperature intensity  $(T'^2)^{1/2} / (T_1 - T_2)$ . As noted previously,  $\sigma_\psi$  is nearly constant across the central regions of the jet,  $\sigma_\psi \approx 0.15$ .

If one neglects boundary effects and evaluates the integral of Eq. (26) using Eqs. (27) and (28), then one obtains the following simple closed-form expression for the ensemble average of the reactant  $A$

$$\begin{aligned} \frac{\langle A \rangle}{A_\infty} &= \frac{\bar{X}}{A_\infty} \left\{ \frac{1}{2} \operatorname{erfc} \left[ \frac{-\bar{X}/A_\infty}{2\sigma_\psi^2 [1 + (B_\infty/A_\infty)]^2} \right] \right\} \\ &+ \frac{\sigma_\psi}{(2\pi)^{1/2}} \left( 1 + \frac{B_\infty}{A_\infty} \right) \exp \end{aligned} \quad (29)$$

Specific ensemble average profiles for  $\langle A \rangle / A_\infty$ ,  $\langle B \rangle / A_\infty$ , and  $\langle C \rangle / A_\infty$  have been calculated from Eq. (29) (with  $\sigma_\psi = 0.15$ ) and are shown plotted in Figs. 7 and 8. Each figure presents results corresponding to a different mixture ratio  $B_\infty / A_\infty (=1, 4)$  and compares the ensemble-average solutions (solid lines) with results that one would obtain with an

equivalent laminar flame<sup>††</sup> sheet model. Note the rounded peak in the  $\langle C \rangle$  profile which moves to the  $A$  side of the jet when  $B_\infty/A_\infty > 1$ , and to the  $B$  side when  $B_\infty/A_\infty < 1$ . For mixture ratios much different from unity, the flame sheet location may be close to the jet boundaries, in which case the Gaussian pdf model is no longer valid.

The equivalent laminar flame sheet model predicts a maximum value of  $\bar{C}$  at the average flame sheet location  $\bar{X}=0$  given by

$$C_{\max, \sigma_\psi=0} = \bar{\psi}_{\bar{X}=0} = (B_\infty/A_\infty) / (1 + B_\infty/A_\infty) \quad (30)$$

The equivalent laminar solution for  $\bar{A}$ , presented in Figs. 7 and 8, requires that  $\bar{A}$  decrease linearly from its freestream value  $A_\infty$  (at  $\eta=1.4$ ) and vanish at the average flame sheet location,

$$\eta_{\text{av flame}} = 1.6 - [3.0(B_\infty/A_\infty) / (1 + B_\infty/A_\infty)] \equiv \eta_F \quad (31)$$

The ensemble average solution for  $\langle C \rangle$  shows a marked reduction and broadening of the  $\langle C \rangle$  profile, in the region near the average flame sheet location  $\eta_F$ , when compared to the equivalent laminar solution. The peak ensemble average for  $C$  at  $\eta_F$  is given simply by

$$\langle C \rangle_{\eta_F} = \frac{B_\infty/A_\infty}{(1 + B_\infty/A_\infty)} - \frac{\sigma_\psi(1 + B_\infty/A_\infty)}{(2\pi)^{1/2}} \quad (32)$$

For  $\sigma_\psi=0.15$  and  $B_\infty/A_\infty=1$ , Eqs. (20) and (32) show a maximum 24% reduction in  $\langle C \rangle$  from that given by the equivalent laminar solution, Eq. (30). For a  $B$  "rich" flow,  $B_\infty/A_\infty=4$ , the reduction is 37%. The net flux of  $\langle C \rangle$  given by

$$\begin{aligned} \langle \dot{C} \rangle &= \int_{-\infty}^{\infty} \bar{u} \langle C \rangle dy \\ &= \frac{\bar{u}_1 \langle C \rangle_{\max} \cdot x}{\sigma_u} \int_{-\infty}^{\infty} \left[ \frac{\bar{u}}{u_1} \right] \frac{\langle C \rangle}{\langle C \rangle_{\max}} d\eta \end{aligned} \quad (33)$$

will be reduced by approximately 5% [for  $B_\infty/A_\infty=1$ ] from the levels predicted by the equivalent laminar solution. The reduction in  $\langle C \rangle$  increases in magnitude for non-stoichiometric conditions [ $B_\infty/A_\infty \rightarrow \infty$  or  $B_\infty/A_\infty \rightarrow 0$ ]. For higher fluctuation levels in the passive species intensity  $\sigma_\psi$ , the maximum level of  $\langle C \rangle$  will be reduced further.

The preceding results must be kept in mind if one seeks to improve the output of a chemical laser by increasing the turbulent mixing in the reactive jet by some artificial means (such as a wire trip). For if, in the process of increasing the spreading rate [lowering  $\sigma_u$  in Eq. (33)], the large-scale fluctuations generated by the external source introduce greater rms fluctuations in the passive species [increasing  $\sigma_\psi$  in Eq. (32)], then part of the benefit of a greater overall spreading rate will be lost because of the reduction in the amount of  $\langle C \rangle$  resulting from the turbulent inhomogeneities induced in the reacting species field.

Not only does the ensemble average for  $C$  differ significantly from the equivalent laminar flame sheet solution, but so do the ensemble averages for the reactants  $A$  and  $B$  (see Figs. 7 and 8).  $\langle A \rangle$ , instead of vanishing at the average flame sheet location  $\eta_F$ , is seen to extend below  $\eta_F$ , tapering off gradually to zero in the region where the ensemble average value of  $\langle B \rangle$  is nonzero. The effective turbulent diffusion flame thus has a thickness approximately one-third the scale of the shear layer width centered near  $\eta_F$ . This effective broadening of the reaction zone for turbulent diffusion

<sup>††</sup>The terminology "equivalent laminar flame" refers to a mixing layer with a spreading rate equal to that of a turbulent layer, but with no species fluctuations, i.e.,  $\sigma_\psi=0$ .

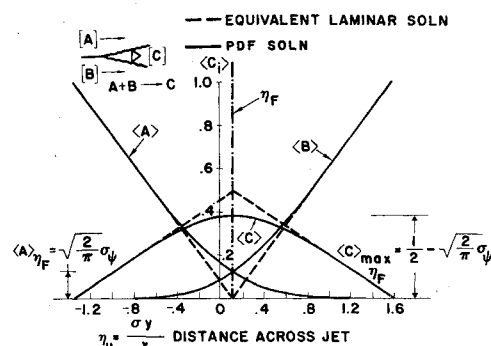


Fig. 7 Ensemble average of reactants and products ( $B_\infty/A_\infty=1$ ),  $\sigma_\psi=0.15$ .

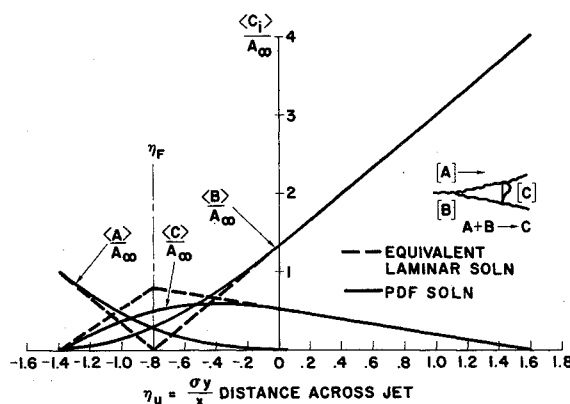


Fig. 8 Ensemble average of reactants and products ( $B_\infty/A_\infty=4$ ),  $\sigma_\psi=0.15$ .

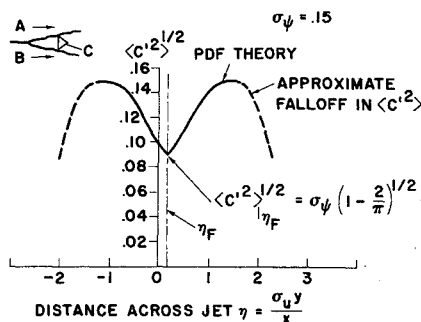


Fig. 9 Root-mean-square products fluctuation levels  $\langle C'^2 \rangle^{1/2}/A_\infty$  ( $B_\infty/A_\infty=1$ ),  $\sigma_\psi=0.15$ .

flames has been seen previously in the measurements of Hawthorne et al.<sup>11</sup>

An additional measure of the effect of the scalar turbulence level on the reacting flowfield is the rms fluctuation levels of the product of reaction, i.e.,  $\langle C'^2 \rangle$ . Fluctuations in  $C$  may affect the quality of a chemical laser output signal.  $\langle C'^2 \rangle$  is calculated from the following expressions related to the second moment of  $C$

$$\langle C'^2 \rangle = \langle C^2 \rangle - \langle C \rangle^2 \quad (34)$$

where

$$\langle C^2 \rangle = \langle \psi'^2 \rangle + \langle \psi \rangle^2 - 2\langle \psi A \rangle + \langle A^2 \rangle \quad (35)$$

In Eq. (35), the terms  $\langle \psi'^2 \rangle = \sigma_\psi^2 A_\infty^2$  and  $\langle \psi \rangle^2$  all are evaluated readily from the properties of the scalar field.  $\langle A^2 \rangle$  is determined from the second moment of the distribution function

$$\langle A^2 \rangle = \int_0^\infty X^2 f(X) dX \quad (36)$$

The cross-correlation term  $\langle \psi A \rangle$  is defined as

$$\langle \psi A \rangle = \int_0^\infty \psi(X) X f(X) dX \quad (37)$$

To evaluate Eq. (37), an assumption must be made about the relationship between instantaneous local values of the scalars  $\psi$  and  $X$ . It is assumed that the relation between  $\psi$  and  $X$  is identical to that of their means, or

$$(X + B_\infty) / (A_\infty + B_\infty) = \psi / A_\infty \quad (38)$$

This assumption is completely true only if the molecular diffusivities of the system are equal.

A plot of  $\langle C'^2 \rangle$  calculated from Eq. (34) is presented in Fig. 9 for the case  $B_\infty / A_\infty = 1$ . It is seen that the intensities of the  $C$  fluctuations are a minimum at the center of the reaction zone, the magnitude at this location being

$$(\langle C'^2 \rangle / A_\infty^2)^{1/2} = \sigma_\psi [1 - (2/\pi)]^{1/2} \quad (39)$$

or

$$\langle C'^2 \rangle^{1/2} / A_\infty \approx 0.09 \quad \text{if } \sigma_\psi = 0.15, \quad B_\infty / A_\infty = 1$$

Away from the reaction zone, the fluctuations in  $C$  approach the fluctuation levels for the passive species, i.e.,  $\langle C'^2 \rangle^{1/2} \rightarrow \sigma_\psi$ . As shown in Ref. 3, one finds that the passive species fluctuation levels drop rapidly to zero at the outer edges of the jet. This edge effect on the  $C$  profile is indicated by the dashed lines in Fig. 9. Thus, for the case  $B_\infty / A_\infty = 1$ , the overall  $\langle C'^2 \rangle^{1/2}$  profile is predicted to be double-humped, with the peak levels occurring near the upper and lower boundaries of the shear layer. Whether this fluctuation level distribution is evidenced in chemical laser or other diffusion flame measurements awaits further investigation.

## V. Conclusions

By postulating a single variate normal distribution for the probability density function of the passive field, with mean and variance given by the scalar analysis, simple integral expressions were derived for the mean and rms fluctuation levels of the products of chemical reactions. The principal conclusions for  $N_2O_4 + N_2 = 2NO_2 + N_2$  are as follows:

1) For primary stream temperatures near  $T_1 \approx 252K$ , the ratio of chemical to turbulent diffusion times is very small,  $\tau_c / \tau_D < 0.01$ . Hence, one can assume that nearly all size eddies in the flow are in a state of local chemical equilibrium.

2) A local equilibrium model, based on the mean temperature ( $\bar{T}$ ) only, can lead to an overestimate of the peak concentration of mean  $NO_2$  (of from 5 to 15%) compared to the results of the ensemble average theory,  $\langle NO_2 \rangle$ , which accounts for the statistical behavior of the random equilibrium eddies. The ensemble mean results are in reasonable agreement with Batt's data for  $NO_2$ .

3) Calculated profiles of  $(NO_2'^2)^{1/2} / [NO_2]_1$  indicate very large intensities, ranging from 30 to 100% as primary temperatures  $T_1$  decrease from 252 to 220 K. The pdf calculated intensity results for the  $T_1 = 252$  K case are in substantial

agreement with Batt's data and with a local equilibrium calculation using direct temperature time traces.

For  $A + B \rightarrow C$ , these conclusions are reached:

1) Unlike laminar flame sheet theory, a wide turbulent diffusion flame is formed centered near the average flame location, having a thickness approximately one-third the scale of the shear layer width, with the ensemble average of  $\langle A \rangle$  being nonzero in regions where  $\langle B \rangle$  is nonzero, and vice versa.

2) The peak ensemble averages for the product of reaction  $\langle C \rangle$  are reduced on the order of 20 to 40% (depending on the mixture ratio  $B_\infty / A_\infty$ ) over what would have been predicted from an equivalent laminar flame theory.

3) For the case of equal freestream concentrations ( $B_\infty / A_\infty = 1$ ), the rms fluctuation distribution of  $C$  across the jet is calculated to be double-humped, with a minimum value of  $\langle C'^2 \rangle^{1/2}$  at the average flame sheet location.

4) The analysis indicates for the chemical laser that the beneficial performance effects of increased mixing layer spreading rates, created, say, by an artificial trip, will be reduced to some degree by increasing scalar fluctuation intensities generated in the mixing region.

## References

- Batt, R. G., "Turbulent Chemical Kinetics Investigation," P.S.S. III, Task 4.11 Final Rept., SAMSO TR 74-62, Rept. 18117-6023-RU-00, Feb. 1974, TRW; also Batt, R.G., Kubota, Ta., and Laufer, J., "Experimental Investigation of the Effect of Shear Flow Turbulence on a Chemical Reaction," AIAA Paper 70-721, June 1970, San Diego, Calif.
- Hofland, R. and Mirels, H., "Flame Sheet Analysis of C.W. Diffusion-Type Chemical Laser, I. Uncoupled Radiation," *AIAA Journal*, Vol. 10, No. 4, April 1972, pp. 420-428.
- Alber, I.E. and Batt, R.G., "An Analysis of Diffusion Limited First and Second Order Chemical Reactions in a Turbulent Shear Layer," AIAA Paper 74-593, June 1974, Palo Alto, Calif.
- O'Brien, E.E., "Turbulent Mixing of Two Rapidly Reacting Chemical Species," *Physics of Fluids*, Vol. 14, No. 7, July 1971, pp. 1326-1331.
- Toor, H.L., "Mass Transfer in Dilute Turbulent and Non-turbulent Systems with Rapid Irreversible Reactions and Equal Diffusivities," *American Institute of Chemical Engineering Journal*, Vol. 8, No. 1, March 1962, pp. 70-78.
- Chung, P.M., "On the Development of Diffusion Flame in Homologous Turbulent Shear Flows," AIAA Paper 70-722, June 1970, San Diego, Calif.
- Libby, P.A., "On Turbulent Flows with Fast Chemical Reactions Part III—Two Dimensional Mixing with High Dilute Reactants," Oct. 1973, University of California, San Diego, Calif. (to be published).
- Carington, T. and Davidson, N., "Shock Waves in Chemical Kinetics: The Rate of Dissociation of  $N_2O_4$ ," *Journal of Physical Chemistry*, Vol. 57, No. 4, April, 1953, pp. 418-427.
- Bodenstein, M., "Bildung und Zersetzung der hohen Stickoxyde," *Zeitschrift für Physikalische Chemie*, Vol. 100, 1922, p. 68; also Wegner, P.P., "Supersonic Nozzle Flow with a Reacting Gas Mixture," *Physics of Fluids*, Vol. 2, No. 3, May-June 1959, pp. 264-275.
- Bilger, R.W., "The Structure of Diffusion Flames," 1975, (submitted for publication).
- Hawthorne, W.R., Wedell, D.S., and Hottel, H.C., "Mixing and Combustion in Turbulent Gas Jets," *Third Symposium on Combustion Flame and Explosion Phenomena*, 1949, pp. 267-300.